BBA - Molecular Basis of Disease 1865 (2019) 512–524

Contents lists available at ScienceDirect

BBA - Molecular Basis of Disease

journal homepage: www.elsevier.com/locate/bbadis

Enhanced remedial effects for vitamin D_3 and calcium co-supplementation against pre-existing lead nephrotoxicity in mice: The roles of renal calcium homeostatic molecules

Riyad A. Almaimani[a,1], Hussain Almasmoum[b], Mazen M. Ghaith[b], Mohamed El-Boshy[b,c], Shakir Idris[b], Jawwad Ahmad[b], Abdelghany H. Abdelghany[b,d], Mohammad A. BaSalamah[e], Amani Mahbub[b], Bassem Refaat[b,*,1]

[a] Biochemistry Department, Faculty of Medicine, Umm Al-Qura University, Al Abdeyah, PO Box 7607, Makkah, Saudi Arabia
[b] Laboratory Medicine Department, Faculty of Applied Medical Sciences, Umm Al-Qura University, Al Abdeyah, PO Box 7607, Makkah, Saudi Arabia
[c] Department of Clinical Pathology, Faculty of Veterinary Medicine, Mansoura University, Mansoura, Egypt
[d] Department of Anatomy, Faculty of Medicine, Alexandria University, Alexandria, Egypt
[e] Pathology Department, Faculty of Medicine, Umm Al-Qura University, Al Abdeyah, Makkah, Saudi Arabia

ARTICLE INFO

Keywords:
TRPV5
TRPV6
Voltage-dependent calcium channels
Calbindin
Calmodulin
CAMKII

ABSTRACT

Background: Lead (Pb) is a toxic heavy metal and nephropathy is common with chronic exposure. Although vitamin D (VD) and calcium (Ca) showed promising protections, their co-administration was not previously investigated in Pb nephrotoxicity. This study measured the potential interactions and remedial effects of VD and/or Ca on established Pb nephropathy.

Methods: Fifty adult male mice were equally distributed into: negative controls (NC), positive controls (PC), Ca, VD and VDC groups. The study duration was seven weeks and all groups, except the NC, received Pb acetate in drinking water (500 mg/L) throughout the study. The Ca, VD and VDC groups also received oral Ca (50 mg/kg; five times/week) and/or intramuscular VD (1000 IU/kg; three times/week) from week four till the end of the study.

Results: The PC group showed substantial reduction in serum VD, hypocalcaemia, hypercalciuria and proteinuria alongside marked tissue inflammation, oxidative stress and apoptosis/necrosis. Pathological alterations were also detected in the mRNAs and proteins of the VD-metabolising enzymes, receptor and binding protein alongside several Ca-membrane channels, membrane transporters, intracellular binding proteins and mediators. While both monotherapies equally demonstrated moderate improvements, the VDC showed the utmost corrective actions on serum and tissue Pb concentrations, the inflammatory and antioxidative markers, the expressions of renal VD/Ca-molecules and tissue integrity. Moreover, the results were comparable between the VDC and NC groups.

Conclusions: This report is the first to reveal potential enhanced remedial outcomes for combining VD and Ca against pre-existing Pb nephrotoxicity and the enhancements could be dependent on Ca-regulatory pathways.

1. Introduction

Lead (Pb) is a divalent heavy metal that persistently pollutes the environment and chronic toxicity usually occurs by ingestion and inhalation [1,2]. Prolonged exposure to Pb causes adverse health effects and a recent study has reported that high blood Pb levels (BLL) accounted for > 400,000 annual deaths and a 37% increase in all-cause mortality in the United States [3]. Chronic Pb toxicity induces tissue injury typically by provoking a T-helper (Th)2 proinflammatory immune response characterised by upregulations in the expressions of interleukin (IL)1β and IL6, and the inhibition of IL10 and interferon (IFN)-γ [4,5]. Pb also promotes oxidative stress in targeted tissues by inhibiting the antioxidant enzymes, increasing the production of reactive oxygen species (ROS), promoting lipid peroxidation and DNA

* Corresponding author at: Laboratory Medicine Department, Faculty of Applied Medical Sciences, Umm Al-Qura University, Holy Makkah, PO Box 7607, Saudi Arabia.
E-mail address: bassem.refaat@yahoo.co.uk (B. Refaat).
[1] These authors contributed equally to the work.

https://doi.org/10.1016/j.bbadis.2018.11.023
Received 16 August 2018; Received in revised form 9 November 2018; Accepted 24 November 2018
Available online 12 December 2018

damage [6–8]. Blood Pb is mainly eliminated by renal filtration and tubular secretion. Hence, chronic Pb toxicity is commonly associated with nephropathies and the renal pathologies encompass diminished glomerular filtration rate (GFR), tubular atrophy, interstitial fibrosis and chronic renal failure [9–11].

The kidney is a key regulator of calcium (Ca^{2+}) homeostasis by activating vitamin D (VD) and reabsorbing 99% of filtrated Ca^{2+} by renal tubules [12,13]. VD is a calciotrophic steroid hormone that controls duodenal absorption and renal reabsorption of Ca^{2+} [14,15]. VD is initially formed in the skin as a pro-hormone and the active form (VD_3) is later produced in the kidney by the synthesising enzyme Cyp27b1 [14]. VD circulates bound to its binding protein (VDBP), triggers its cellular signals through its nuclear receptor (VDR) and the hormonal actions are regulated by the catalysing enzyme Cyp24a1 [15,16]. VD induces the absorption of Ca^{2+} from the lumenal surface of the intestinal tract and renal tubules by upregulating the transient receptor potential cation channel subfamily V members (TRPVs) 5 and 6, which are highly selective for Ca^{2+} [17–19]. VD also upregulates the cytosolic VD-dependent Ca^{2+} binding proteins, calbindin-D_{28k} (CALB1) and calbindin-D_{29k} (CALB2), to shuttle Ca^{2+} from the lumenal border towards the cellular basolateral membrane [20,21].

The influx of Ca^{2+} occurs through several membrane ionic channels including the voltage-dependent Ca^{2+} channels (VDCCs) [17,22]. These channels are classified according to the voltage-gradient required for their activation and the transient (T)-type is activated by low-voltage gradient, whereas a high-voltage gradient is needed for activating the long-lasting (L)-type [17,22,23]. In the cytosol, free Ca^{2+} binds to calmodulin (CAM) that subsequently activates the Ca^{2+}/CAM-dependent kinase II (CAMKII) family of protein kinases to regulate critical cellular functions including muscle contraction, neurotransmission, gene expression, inflammation, apoptosis, and immune response [1,24,25].

Pb toxicity is associated with significant dysregulations in the VD-Ca^{2+} axis and several population-based studies have shown negative correlations between the serum levels of VD and/or Ca^{2+} with BLL [26,27]. Moreover, consuming Ca^{2+} above the Dietary Reference Intake induced significant declines in BLL [28–32]. At the molecular level, Pb disrupts the Ca^{2+}-signalling pathways through a process known as ionic displacement or ionic mimicry [2,24]. Pb occupies the extracellular binding-domain of the VDCCs, thus resulting in their inhibition [33–36]. Pb also replaces Ca^{2+} in many of its intracellular binding proteins (CaBPs) and CAM has higher binding affinity to Pb than Ca^{2+} [25,36]. Pb also negatively modulates the VD regulatory proteins in a broad range of organs, including the kidney [10,37].

Ca^{2+} is involved in many molecular pathways associated with the regulation of renal glomerular and tubular functions [38,39]. The $Ca_v3.1$ and $Ca_v3.2$ T-types and the $Ca_v1.2$ L-type VDCCs are expressed in the glomerular vessels, and they regulate the GFR [17,22,23]. Ca^{2+} also regulates many of the renal cellular functions through the CAM/CAMKII pathway [38,40]. Nonetheless, the pathogenic mechanisms underlying Pb nephropathy in addition to the potential interactions between Pb and renal Ca^{2+}-homeostatic molecules are currently not fully understood [1,8,12]. On the other hand, we have previously shown the nephroprotective properties of prophylactic VD_3 against Pb nephrotoxicity [10]. Furthermore, recent randomised placebo-controlled clinical trials (RCT) have also reported enhanced anti-inflammatory and antioxidative outcomes for co-supplementing VD with Ca^{2+} [41–44]. Therefore, this study was designed to measure the potential interactions between renal VD/Ca^{2+}-homeostatic molecules with Pb nephrotoxicity as well as the therapeutic effects of Ca^{2+} and/or VD_3 supplementations against Pb nephropathy established prior to treatment initiation.

2. Materials and methods

2.1. Study design and treatment protocols

Approval from the Committee for the Care and Use of Laboratory Animals at Umm Al-Qura University was obtained prior to the initiation of animal experimentation (AMSEC 16/19-09-17). Lead acetate trihydrate of 99.99% purity (Sigma-Aldrich Co.; MO, USA), calcium carbonate tablets containing 600 mg of elemental calcium (CALCINATE®; Riyadh Pharma, Riyadh, Saudi Arabia) and vitamin D_3 intramuscular (IM) ampoules containing 100,000 IU/ml (Devarol-S; Memphis Co. for Pharm. & Chem. Ind., Cairo, Egypt) were used.

Fifty BALB/c male mice of 16 weeks of age and 25–30 g of body weight each were housed in clean and sterile polyvinyl cages (5 mice/cage) and kept in controlled temperature (22–24 °C) and 12 h dark/light cycle. The mice were maintained on a standard laboratory pellet diet that contained 2000 IU/Kg VD_3 and 0.70% $CaCO_3$. The animals were allocated randomly and equally into five groups (10 mice/group) as follow: the negative control (NC) group, positive control (PC) group, monotherapy with either Ca^{2+} (Ca group) or VD_3 (VD group) and the dual therapy group that was simultaneously treated with VD_3 and Ca^{2+} (VDC group). Pb was dissolved in the drinking water (500 mg/L) of all groups, except the NC, and the animals had free access to water throughout the total study duration of 7 weeks [12,45–47]. Since the oral LD_{50} has not been previously reported, the applied concentration of Pb acetate (75 mg/Kg/day) was equal to 53.6% of the intraperitoneal (140 mg) and 72.1% of the intravenous (104 mg/Kg) LD_{50} doses [47]. Treatment with IM VD_3 (1000 IU/kg; three times/week) and/or oral elemental Ca^{2+} (50 mg/kg; five times/week) started in the fourth week and lasted for the remaining four weeks, as previously described [10,48]. According to the dose conversion equation between mouse and human [49], the total amount of VD_3 (54.3 IU/Kg/day) and Ca^{2+} (37 mg/Kg/day) received by the treated groups from diet and therapeutic regimens were equal to 1.8-fold the daily requirements of VD_3 (1750 IU/day [range 1500–2000 IU/day]; 29.1 IU/Kg/day) and Ca^{2+} (1000 mg/day; 16.7 mg/Kg/day) for an adult human of 60 Kg body weight.

2.2. Types of samples

The animals from each group were individually housed in a separate Techniplast® metabolic cage (Braintree Scientific, Inc.; MA, USA) a day prior to euthanasia to collect 24-hour urine samples. Diethyl ether (Fisher Scientific UK Ltd.; Loughborough, UK) was used for anaesthesia and 1 ml of blood was obtained from each mouse in a plain tube from the middle canthus of the eye just before euthanasia. Serum was collected by centrifugation and then stored in −20 °C.

Both kidneys from each animal were harvested, cut in halves and one portion was then processed by conventional methods prior to embedding in paraffin. Another half was digested with 6:1 wet acid ultrapure concentrated nitric acid: Perchloric acid using a Microwave Digestion System. The digested samples were then diluted with ultrapure deionized water and processed to measure Pb concentrations. The third half (0.2 g) was placed in 1 ml of RIPA lysis buffer containing protease inhibitors (Santa-Cruz Biotechnology Inc.; CA, USA) for total protein extraction. The concentrations of renal total proteins were measured in the resultant supernatants by Pierce™ Rapid Gold BCA Protein Assay Kit (Thermo Fisher Scientific; CA, USA). The samples were then diluted with ultrapure deionized water for a final concentration of 1000 μg/ml or 2000 μg/ml to be used for ELISA and Western blot, respectively. The residual renal specimens were immersed in RNA*later* (Thermo Fisher Scientific) and stored in −80 °C. Total RNA was extracted using the Paris kit (Thermo Fisher Scientific) according to the manufacturer's instructions. RNA quality was assessed by a BioSpec-nano instrument (Shimadzu Corporation; Tokyo, Japan) and the quantities were determined by Qubit Fluorometer (Thermo

Fisher Scientific).

2.3. Lead concentrations in serum, renal tissue and urine samples

The concentrations of serum, urine and renal tissue Pb were measured by atomic absorption spectrophotometry (Perkin Elmer AAnalyst 800; MA, USA) with hollow cathode lamp of Pb at wavelength of 283.3 nm as previously described [10].

2.4. Serum and urine biochemical parameters assays

The serum levels of renal function markers (creatinine, urea, total protein and albumin), 25-OH vitamin D and liver enzymes in addition to the concentrations of total protein in the 24-hour urine samples were measured on Cobas e411 (Roche Diagnostics International Ltd.; Risch-Rotkreuz, Switzerland) according to the manufacturer's protocols.

2.5. Enzyme linked immunosorbant assay (ELISA)

The serum, urine and renal tissue calcium concentrations were determined by a colorimetric calcium assay kit (Cayman Chemical Co.; MI, USA). The concentrations of IL1β, IL6, IL10, and IFN-γ in renal tissue lysate were measured using specific mouse ELISA kits (Cloud-Clone Corp.; TX, USA). The antioxidative markers glutathione (GSH), catalase (CAT), glutathione peroxidase (GPx) and the lipid peroxidation marker, malondialdehyde (MDA), were also measured in renal tissue by ELISA (Cayman Chemical Co.). All samples were processed in duplicate on a fully automated ELISA system (Human Diagnostics; Wiesbaden, Germany) and according the manufacturers' guidelines.

2.6. Western blot

The renal protein expressions of Cyp27b1, Cyp24a1, VDBP, VDR, caspases (CASP)-3, -8 & -9, CALB1 & 2, TRPV5 & 6, the $Ca_v3.1$ and $Ca_v1.2$ channels, CAM and CAMKIIA were measured by Western blot. Goat primary polyclonal IgG antibodies were used for the detection of Cyp27b1 and Cyp24a1 (Santa-Cruz Biotechnology Inc.), while those against cleaved Casp-3, $Ca_v1.2$, CAM and TRPV6 were mouse monoclonal antibodies (Thermo Fisher Scientific). The remaining primary IgG antibodies were rabbit polyclonal and were from Santa-Cruz Biotechnology Inc. for VDR and VDBP, Cloud-Clone Corp. for Casp-8 & -9, CALB1 & 2, and Thermo Fisher Scientific for $Ca_v3.1$, TRPV5 and CAMKIIA. β-actin loading control mouse monoclonal antibody (Thermo Fisher Scientific) was used for normalisation.

Renal tissue lysates containing 20 µg of total proteins each were resolved by electrophoresis using gradient 4–20% Mini-PROTEAN® TGX Stain-Free™ SDS-PAGE gels (Bio-Rad Laboratories Inc.; CA, USA). The proteins were then transferred on Trans-Blot® Turbo™ Mini 0.2 µm PVDF membranes using a Trans-Blot® Turbo™ Transfer System (Bio-Rad Laboratories Inc.). The membranes were blocked for 60 min with Tris-buffered saline (TBS) buffer containing 5% non-fat dry milk (Santa-Cruz Biotechnology Inc.) and then incubated with the primary antibodies overnight at 4 °C. The dilutions of the primary antibodies were 1:1000 for Cyp24a1, VDBP, VDR, $Ca_v1.2$, $Ca_v3.1$, CAM and CAMKIIA, and 1:500 for the remaining antibodies. The membranes were washed with TBS-Tween (3 × 5 min) and then incubated with the corresponding highly cross-adsorbed and HRP-conjugated donkey anti-mouse, anti-goat or anti-rabbit secondary antibodies (Thermo Fisher Scientific) for 60 min at room temperature and 1:10,000 final concentration. The membranes were developed using Pierce ECL Plus-kit (Thermo Fisher Scientific). Blots were scanned using ChemiDoc™ XRS + System (Bio-Rad Laboratories Inc.) and the quantification of band density was calculated on ImageJ software (https://imagej.nih.gov/ij/) followed by normalisation against the densitometry of the corresponding β-actin band, as previously described [50].

2.7. Immunofluorescence staining

The co-localisation of $Ca_v3.1$ with $Ca_v1.2$ calcium channels and CAM with CAMKIIA in renal tissues was done by using primary monoclonal mouse ($Ca_v1.2$ & CAM) and polyclonal rabbit ($Ca_v3.1$ & CAMKIIA) IgG antibodies. Briefly, all slides were simultaneously incubated with a mixture of the corresponding primary mouse and rabbit antibodies at 1:150 concentration for 3 h after blocking with normal donkey serum. Slides were then incubated for 60 min with a mixture of highly Cross-adsorbed tagged secondary donkey anti-rabbit (Alexa Fluor™ 555) and anti-mouse (Alexa Fluor™ 488) IgG antibodies (Thermo Fisher Scientific). Sections were finally counterstained with ProLong Diamond Anti-fade Mountant containing DAPI (Thermo Fisher Scientific). All slides were examined on an EVOS FL microscopy (Thermo Fisher Scientific) and digital images were captured within the same session from 10 random non-overlapping fields from each slide using 40× objective.

2.8. TUNEL assay

Cell DNA damage and cell apoptosis/necrosis were assessed in the collected renal specimens by the Click-iT™ TUNEL Alexa Fluor™ 488 Imaging Assay (Thermo Fisher Scientific) and by following the manufacturer's protocol. Additionally, a sequential protocol was applied to co-localise cleaved Casp-3 with the apoptotic bodies. Following the completion of the TUNEL protocol, all slides were immediately incubated with the primary mouse monoclonal IgG antibody against Casp-3 at 1:100 concentration for 3 h. The slides were then washed for 10 min in TBS-Tween and were incubated with highly Cross-adsorbed tagged secondary donkey anti-mouse (Alexa Fluor™ 555) IgG antibodies (Thermo Fisher Scientific). Sections were finally counterstained and mounted as described above. Stained slides were examined on an EVOS FL microscopy at 40× magnification. DNA damage was indicated by the emission of green fluorescence dye and the apoptosis index was calculated by counting the percentage of apoptotic/necrotic cells in 15 random non-overlapping fields from each tissue section using the cell counter tool provided with the microscope software as previously described [51].

2.9. Quantitative RT-PCR

The cDNA was synthesised from 200 ng total RNA using a high capacity Reverse Transcription Kit (Thermo Fisher Scientific). PCR was processed in triplicate wells on ABI® 7500 system and each well contained 10 µl SYBR Green (Thermo Fisher Scientific), 7 µl DNase/RNase free water, 1 µl of each primer (5 pmol; Supplementary Table 1) and 1 µl cDNA (25 ng) and 40 cycles (95 °C/15 s and 60 °C/1 min) of amplification were performed. The negative controls included a minus-reverse transcription control from the previous RT step and another minus-template PCR, in which nuclease free water was used as a template.

The $2^{-\Delta\Delta Ct}$ method was used to perform relative quantitative gene expression of rat *CYP27B1*, *CYP24A1*, *VDR*, *VDBP*, *CACNA1G*, *CACNA1C*, *TPRV5*, *TPRV6*, *CALB1*, *CALB2*, *CALM1*, *CAMK2A*, *Casp3*, *Casp8 and Casp9* genes. Rat *β-actin* gene was used to normalise the Ct values of the genes of interest since it showed the most consistent results among the three tested reference genes. The results are expressed as fold-change compared with the NC group.

2.10. Statistical analysis

SPSS version 16 was used for statistical analysis. All data were assessed for normality by the Kolmogorov and Smirnov's test and homogeneity by Levene test. One-way ANOVA followed by either Tukey's HSD or Games-Howell post-hoc tests were used to compare between the study groups based on variance equality. Correlations were

Table 1
Mean ± SD of lead and calcium concentrations in serum, renal tissue lysate and 24-hour urine samples obtained from the different study groups.

	Pb concentrations			Ca^{2+} concentrations		
	Serum (μg/dl)	Renal tissue (μg/g)	Urine (μg/24-h)	Serum (mg/dl)	Renal tissue (mg/g)	Urine (mg/24-h)
NC group	0.83 ± 0.17	0.16 ± 0.03	ND	10.3 ± 0.52	3.84 ± 0.96	0.38 ± 0.08
PC group	6.25 ± 1.74[b]	9.5 ± 1.56[b]	5.62 ± 1.11[b]	9.02 ± 0.62[b]	1.92 ± 0.48[b]	0.58 ± 0.1[b]
Ca group	5.51 ± 1.15[b]	7.30 ± 1.5[b,c]	5.92 ± 0.71[b]	9.37 ± 0.34[b]	2.72 ± 1.11	0.51 ± 0.08[b]
VD group	4.59 ± 0.83[b,d]	7.95 ± 1.31[b,c]	6.36 ± 0.55[b]	9.54 ± 0.76[a]	3.02 ± 1.23	0.44 ± 0.05[d]
VDC group	1.4 ± 0.33[d,f,g]	2.97 ± 0.6[b,d,f,g]	8.61 ± 1.18[b,d,f,g]	10.24 ± 0.45[d,e]	3.88 ± 0.95[d]	0.43 ± 0.07[d]

ND = Not detected.
[a] P < 0.05 compared with NC group.
[b] P < 0.01 compared with NC group.
[c] P < 0.05 compared with PC group.
[d] P < 0.01 compared with PC group.
[e] P < 0.05 compared with Ca group.
[f] P < 0.01 compared with Ca group.
[g] P < 0.01 compared with VD group.

determined by Pearson's test. P value < 0.05 was considered significant.

3. Results

3.1. Lead and calcium concentrations in serum, renal tissues lysates and urine

The concentrations of Pb increased dramatically, while Ca^{2+} levels were significantly reduced, in the serum and renal tissue lysates of the PC group than the NC group (Table 1). Pb was undetectable in the NC urine samples, but the levels escalated significantly in the PC group simultaneously with a significant elevation in the amount of urine Ca^{+2} compared with the NC group (Table 1). Compared with the PC group, single treatment with Ca^{2+} resulted in a significant decrease only in renal tissue Pb concentrations, whereas VD_3 monotherapy significantly reduced Pb levels in serum and renal tissue lysates. Both monotherapy protocols, however, had no significant effects on Ca^{2+} levels in all sample types, except for VD_3 that significantly lessened the amount of excreted Ca^{2+} in urine (Table 1). Additionally, the Pb concentrations in all sample categories remained significantly higher in both the Ca and VD groups than the NC group and concurred with lower serum Ca^{2+} levels.

On the other hand, the dual therapy resulted in the utmost significant declines in serum and renal tissue Pb levels together with a significant increase in urine Pb concentrations compared with the PC, Ca and VD groups. Additionally, the VDC group had significant increases in serum and renal tissues Ca^{2+} simultaneously with a significant decrease in urine Ca^{2+} compared with the PC group. Nevertheless, Pb concentrations in renal tissue and urine, but not serum, were significantly higher in the VDC group compared with the NC group (Table 1). There was a significant strong positive correlation between Pb concentrations in serum and renal tissue ($r = 0.845$; P < 0.001) along with a moderate significant positive correlation between renal tissue and urine Pb levels ($r = 0.459$; P = 0.001). Significant correlations between Ca^{2+} and Pb levels in all types of samples were also observed (Table 2).

3.2. Serum 25-OH VD and the expression of VD system in renal tissue

Serum 25-OH VD declined significantly in the PC (17.34 ± 4.03 ng/ml; P < 0.001) and Ca (25.09 ± 4.52 ng/ml; P < 0.001) groups compared with the NC group (42.56 ± 3.73 ng/ml). However, the levels were markedly higher in the Ca group than the PC group (P = 0.003). The serum 25-OH VD concentrations were restored in the VD (38.17 ± 5.53 ng/ml) and VDC (43.24 ± 4.11 ng/ml) groups to the NC levels, and they were significantly higher than the PC (P < 0.001 for both) and Ca (P < 0.001 for both) groups. The serum levels of VD also correlated inversely and significantly with the Pb levels in serum ($r = -0.752$; P < 0.001) and renal tissue ($r = -0.785$; P < 0.001) but not with urine Pb levels ($r = -0.145$; P = 0.3).

Table 2
Results of correlation analysis using Pearson's test between Pb and Ca^{2+} concentrations in serum, renal tissue and urine samples.

		Serum Pb (μg/dl)	Renal tissue Pb (μg/g)	Urine Pb (μg/24-h)
Serum Ca^{2+} (mg/dl)	R value	−0.639	−0.760	−0.203
	P value	0.05×10^{-5}	0.01×10^{-8}	0.1
Renal tissue Ca^{2+} (mg/g)	R value	−0.553	−0.705	−0.122
	P value	0.0003	0.01×10^{-5}	0.4
Urine Ca^{2+} (mg/24-h)	R value	0.535	0.727	0.233
	P value	0.0006	0.02×10^{-7}	0.1

In the renal tissue, the PC group had marked reductions in the expression of Cyp27b1 (82%; P = 0.02) and VDR (83%; P < 0.001) mRNAs that also concurred with significant elevations in the Cyp24a1 (2 folds; P < 0.001) and VDBP (> 6 folds; P < 0.001) mRNAs compared with the NC group (Fig. 1A & B). A similar pattern was also observed between the PC and NC groups in the protein expression of Cyp27b1 (51%; P < 0.001), VDR (60%; P < 0.001), Cyp24a1 (1.4 fold; 0.003) and VDBP (4 folds; P < 0.001).

Both monotherapies significantly increased the mRNA and protein of the Cyp27b1 enzyme and paradoxically inhibited those of the Cyp24a1 enzyme and VDBP compared with the PC group (Fig. 1C–E). Furthermore, the mRNA and protein expressions of the VD metabolising enzymes, but not VDBP, were comparable between the NC, Ca and VD groups. VD_3 monotherapy also significantly upregulated the expression of VDR mRNA (9 folds; P < 0.001) and protein (> 2 folds; P < 0.001) than the PC group, whereas the gene and protein expression profiles of VDR were similar between Ca and PC groups (Fig. 1). The combination treatment also induced significant upregulations in the mRNAs and proteins of Cyp27b1 and VDR alongside significant downregulations of the Cyp24a1 and VDBP mRNAs and proteins compared with the PC group. While the expression of Cyp24a1 and VDR were comparable between the VDC and NC groups, the Cyp27b1 and VDBP mRNAs and proteins were significantly elevated in the VDC group (Fig. 1).

3.3. The expression of cellular calcium regulating molecules in renal tissue

3.3.1. Calcium transporting molecules

The mRNAs of TRPV5 (73%; P < 0.001), TRPV6 (64%;

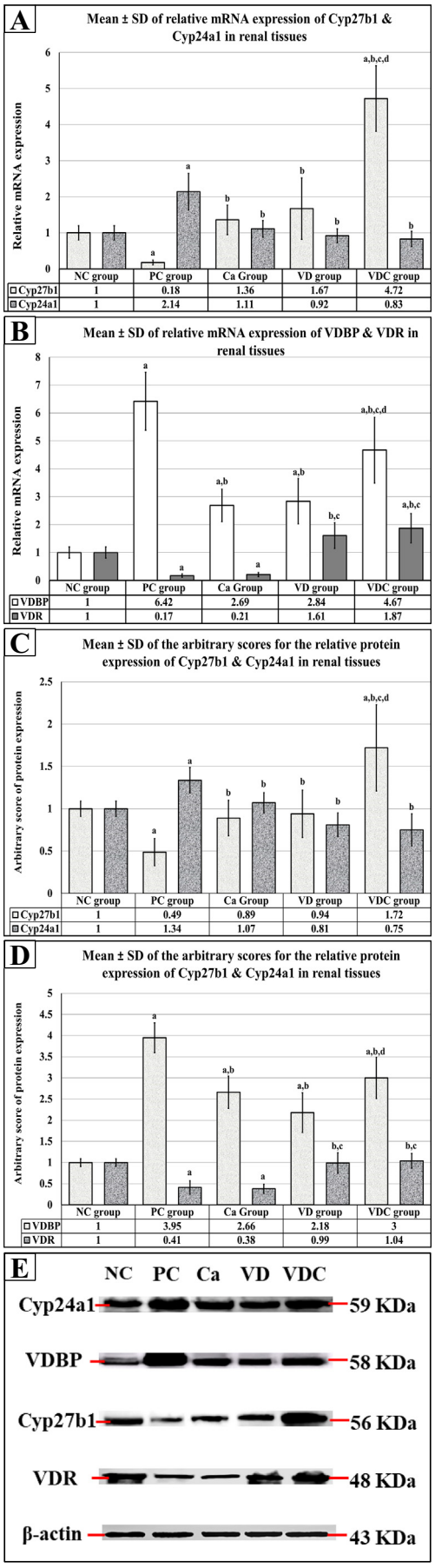

Fig. 1. The mean ± SD of the relative mRNA (A & B) and protein (C & D) expressions of Cyp24a1, Cyp27b1, VDBP & VDR in renal tissue lysates from the different groups together with their (E) protein expressions by western blot. (a = P < 0.05 compared with the NC group; b = P < 0.05 compared with the PC group; c = P < 0.05 compared with Ca group and d = P < 0.05 compared with the VD group).

P < 0.001), CALB1 (78%; P < 0.001) and CALB2 (86%; P < 0.001), were significantly downregulated in the PC group than the NC group (Fig. 2A & B). Similarly, the renal protein expressions of TRPV5 (62%; P < 0.001), TRPV6 (52%; P = 0.01), CALB1 (62%; P < 0.001) and CALB2 (86%; P < 0.001), were significantly diminished in the PC than the NC group (Fig. 2C–E).

The mRNA and protein expressions of TRPV5, TRPV6 and CALB1 in both monotherapy groups were restored to the levels of the NC group and were significantly higher than the PC group (Fig. 2). Although CALB2 mRNA (P = 0.03) and protein (P = 0.005) were also significantly increased in the Ca group compared with the PC group, their levels remained significantly lower than the NC group (P < 0.001 for both). On the other hand, the expressions of CALB2 mRNA and protein in the VD group were equivalent to the NC group and significantly higher than the PC (P < 0.001 for both) and Ca (P < 0.001 for both) groups. Furthermore, the highest mRNA and protein expressions of TRPV5, TRPV6 and CALB1 were observed in the VDC group and were significantly different from all groups (Fig. 2). The CALB2 mRNA and protein were, however, similar between the NC, VD and VDC groups.

3.3.2. *Voltage-dependent calcium channels*

The $Ca_v3.1$ transient (Fig. 3A) and $Ca_v1.2$ long-acting (Fig. 3B) channels in the NC group were co-localised by immunofluorescence in the glomeruli alongside basolateral localisation in renal tubular epithelium. The mRNAs and proteins of both channels decreased significantly in the PC group compared with the NC group (P < 0.001; Fig 3.1 & 2) and both channels were mainly diminished in renal glomeruli and, to a lesser extent, in tubular cells by immunofluorescence (Fig. 3E–H).

Overall, single treatment with Ca^{2+} or VD_3 significantly upregulated the genes and proteins of the VDCCs compared with the PC group (Fig. 3.1–3), and both were mostly localised in the renal tubular cells from the Ca (Fig. 3I–L) and VD (Fig. 3M–P) groups. While the mRNA and protein of $Ca_v1.2$ were comparable between the Ca and NC groups, the $Ca_v3.1$ mRNA (P = 0.001) and protein (P = 0.002) were significantly lower in the former group. Conversely, the expression of both channels was similar between the VD and NC groups. The glomerular expression of the channels was restored in the VDC group and both proteins also showed apical, perinuclear and basal cellular localisation within the renal tubules (Fig. 3Q–T). Additionally, the gene and protein expressions of $Ca_v3.1$ were maximal and significantly different compared with all the study groups (P < 0.001). Nevertheless, the expression of $Ca_v1.2$ in the VDC group was only statistically different than the PC group (Fig. 3.1–3).

3.3.3. *Intracellular calcium signalling molecules*

CAM (Fig. 3a) and CAMKIIA (Fig. 3b) proteins were localised in the cytoplasm and around the nuclei of renal tubular epithelial cells of the NC group by immunofluorescence. Additionally, the gene (Fig. 3.4) and protein (Fig. 3.5 & 6) expressions of CAM and CAMKIIA in the PC group were significantly higher than the NC group (P < 0.001). Both proteins in the PC group also showed basal and paranuclear localisation in the renal tubular epithelium with scarce faint glomerular staining (Fig. 3e–h).

CAM decreased significantly in the Ca group at the gene and protein levels compared with the PC group (P < 0.001) and coincided with a significant decrease in the expression of CAMKIIA mRNA (P = 0.01), but not protein. While CAM mRNA and protein expression levels were

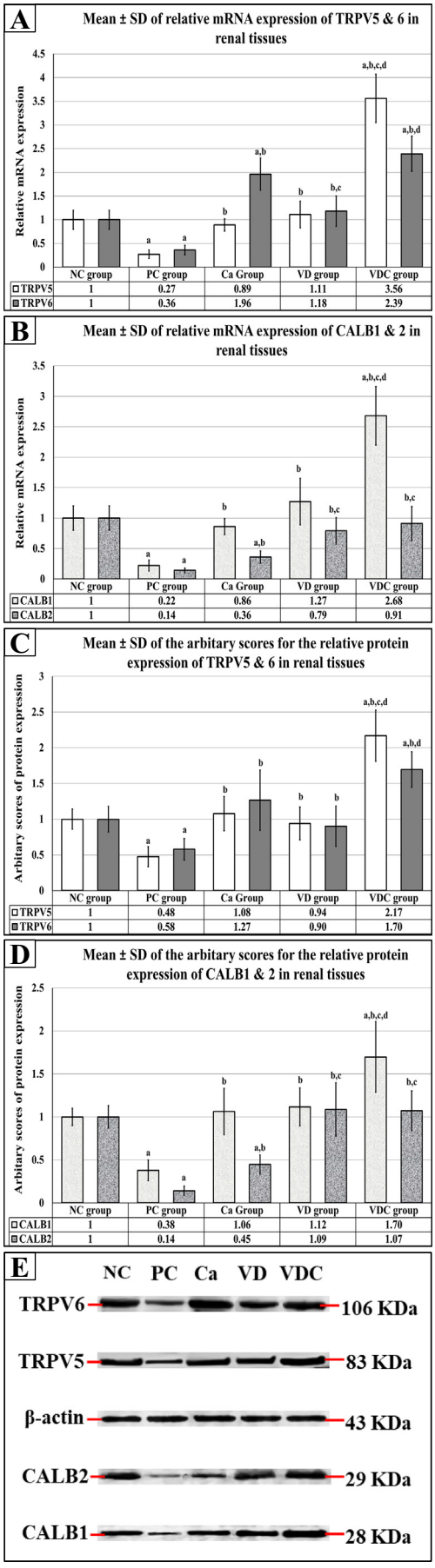

Fig. 2. The mean ± SD of the relative mRNA (A & B) and protein (C & D) expressions of TRPV5, TRPV6, CALB1 & CALB2 in renal tissue lysates from the different groups together with their (E) protein expressions by western blot. (a = P < 0.05 compared with the NC group; b = P < 0.05 compared with the PC group; c = P < 0.05 compared with Ca group and d = P < 0.05 compared with the VD group).

comparable between the Ca and NC groups, the CAMKIIA mRNA and protein were significantly higher in the Ca group. The mRNA and protein expressions of CAM were also significantly inhibited by VD_3 monotherapy compared with the PC group ($P < 0.001$) whereas CAMKIIA mRNA ($P < 0.0001$) and protein ($P = 0.01$) increased significantly in the VD than the PC group. Moreover, CAM and CAMKIIA were significantly higher at the gene and protein levels in the VD group compared with the NC group. Basolateral localisation in the renal tubular epithelium was also observed for CAM and CAMKIIA in the Ca (Fig. 3i–l) and VD (Fig. 3m–p) groups together with more pronounced glomerular staining for CAMKIIA. The VDC group had significantly higher CAM mRNA and protein compared with the NC, Ca and VD groups. CAMKIIA in the VDC group was significantly higher than the NC and PC groups but was comparable to both monotherapy groups (Fig. 3.4–6).

3.4. Renal tissue concentrations of oxidative stress markers and targeted cytokines

The renal tissue concentrations of IL1β and IL6 increased significantly, while those of IL10 and IFN-γ decreased significantly, in the PC group than the NC group (Table 3). Coherently, the tissue levels of the antioxidant markers, GSH, CAT and GPx, were markedly reduced in the PC group and coincided with a significant elevation in MDA compared with the NC group (Table 3). Calcium monotherapy induced significant declines in IL1β and IL6 in addition to a significant increase in IL10 and IFN-γ compared with the PC group. Nevertheless, IL1β and IL6 were significantly higher, while IL10 and IFN-γ were lower, than the NC group. In contrast, the levels of IL1β, IL6 and MDA were significantly diminished, while those of IL10, IFN-γ, GSH, CAT and GPx escalated markedly, in the VD group compared with the PC group. However, significantly higher tissue levels of IL1β and IL6 simultaneously with lower CAT and GPx were detected in the VD group than the NC group (Table 3). The dual therapy protocol, on the other hand, resulted in the greatest significant decreases in IL1β, IL6 and MDA together with the highest significant elevations in IL10, IFN-γ, GSH, CAT and GPx compared with the PC, Ca and VD groups (Table 3).

3.5. Pb-induced renal cell damage and the expression of caspases

The levels of urine total protein together with serum creatinine and urea increased significantly, whereas serum total protein and albumin decreased significantly in the PC group than the NC group (Table 4). While Ca^{2+} monotherapy showed no significant effect on the renal function parameters, VD_3 monotherapy simultaneously increased serum total protein and albumin, and decreased serum creatinine and urine total protein significantly, compared with the PC group. The dual therapy protocol, however, resulted in the highest significant enhancements of all renal biochemical markers compared with the PC group (Table 4). Additionally, the PC group showed abnormal high levels of liver enzymes that were restored to the NC group levels in the VDC group (Supplementary Table 2).

Coherently, very few renal cells from the NC group were positive for apoptosis by the TUNEL technique (Fig. 4A) and simultaneously showed nuclear staining for cleaved Casp-3 (Fig. 4B). The numbers of apoptotic bodies (Fig. 4F) and cells positive for Casp-3 (Fig. 4G) increased dramatically in the tissue sections from the PC group compared with the NC group (Fig. 4.1). Both Ca^{2+} (Fig. 4I–L) and VD_3 (Fig. 4M–P)

T ($Ca_v3.1$) and L ($Ca_v1.2$) voltage-gated calcium Channels

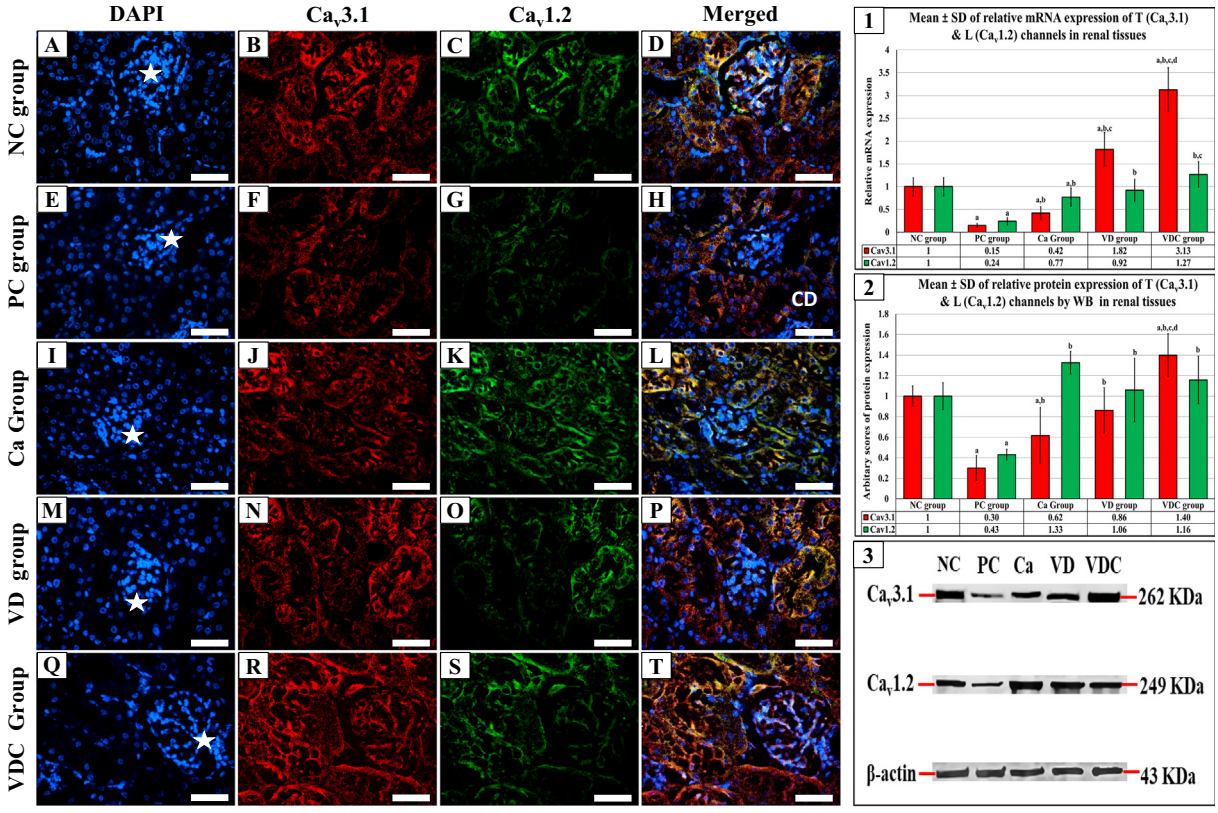

Calmodulin (CAM) & Calmodulin kinase IIα (CAMKIIA)

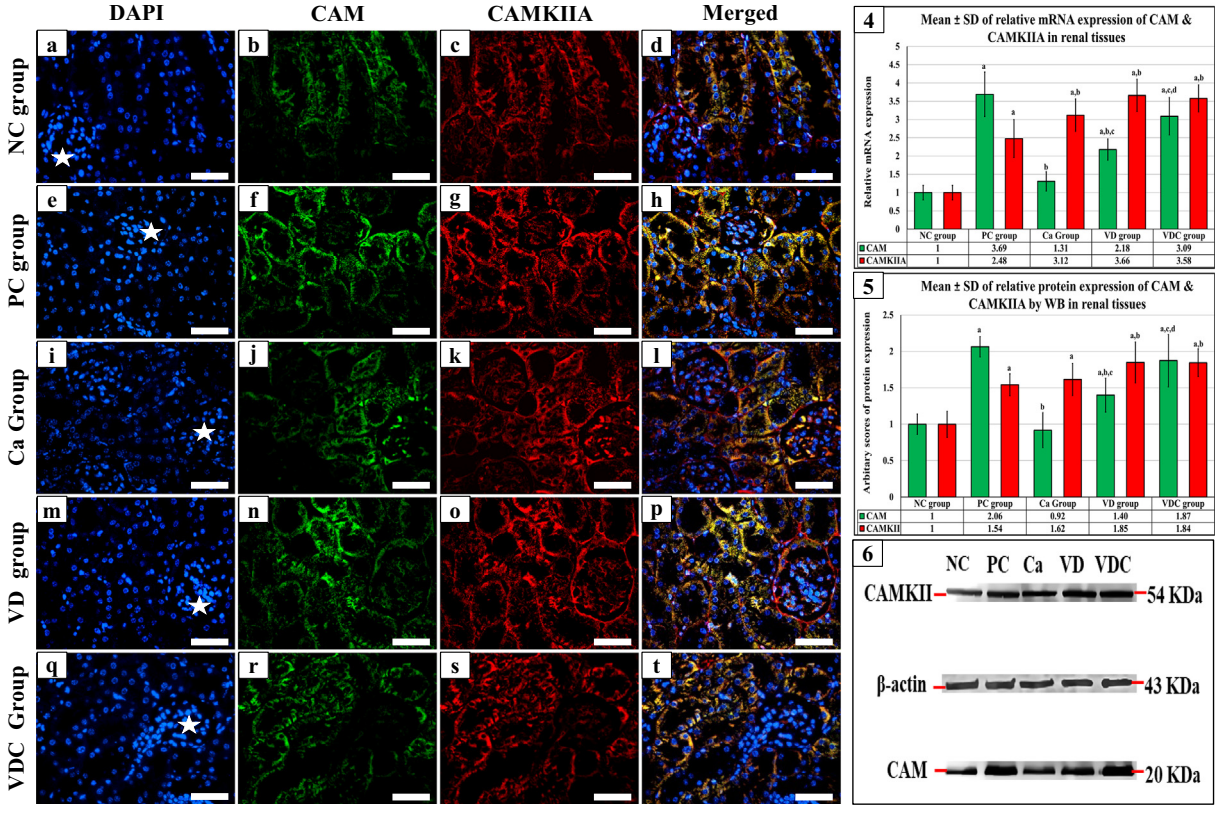

(caption on next page)

Fig. 3. The co-localisation of $Ca_v3.1$ with $Ca_v1.2$ (panels 'A' to 'T') and CAM with CAMKIIα (panels 'a' to 't') in renal tissues are shown by immunofluorescence in the different study groups. All sections were counterstained with DAPI. (40× objective, scale bar = 15 μm and white star = glomerulus). Additionally, the mean ± SD of the relative mRNA and protein expressions of the T-type $Ca_v3.1$ & L-type $Ca_v1.2$ channels (panels 1 & 2) and CAM & CAMKIIA (panels 4 & 5) in renal tissue lysates from the different groups as well as their protein expressions by western blot (panels 3 & 6). (a = $P < 0.05$ compared with the NC group; b = $P < 0.05$ compared with the PC group; c = $P < 0.05$ compared with Ca group and d = $P < 0.05$ compared with the VD group).

monotherapies significantly decreased the numbers of cells positive for apoptosis and Casp-3 compared with the PC group. However, there was no significant difference between the Ca and VD groups, and the numbers of apoptotic bodies were significantly higher in both groups than the NC group (Fig. 4.1). The VDC group showed the utmost significant decline in the apoptosis index compared with the PC, Ca and VD groups (Fig. 4.1). Additionally, the apoptosis index showed strong positive correlations with the levels of serum Pb ($r = 0.863$; $P < 0.001$), renal tissue Pb ($r = 0.942$; $P < 0.001$) and urine Ca^{2+} ($r = 0.753$; $P < 0.001$) together with strong inverse correlations with the levels of serum Ca^{2+} ($r = -0.765$; $P < 0.001$) and 25-OH VD ($r = -0.895$; $P < 0.001$). In agreement with the TUNEL's observations, the mRNA (Fig. 4.2) and protein (Fig. 4.3 & 4) expressions of Casp-8, −9 and −3 were maximal and significantly different in the PC group compared with all study groups ($P < 0.001$). Although all caspases were significantly downregulated by both monotherapies than the PC group, their levels remained significantly higher than the NC group. The Casp-8 and -3 mRNAs and proteins were comparable between the VDC and NC groups whereas Casp-9 was significantly downregulated in the former group (Fig. 4.2 & 3).

4. Discussion

This study measured the interactions between several renal VD/Ca^{2+}-homeostatic molecules and Pb together with the potential remedial effects of VD_3 and/or Ca^{2+} on pre-existing Pb nephropathy. Renal impairment was indicated by the substantial increases of Pb in serum and renal tissue, the pathological alterations in renal function parameters and extensive renal cell apoptosis/necrosis in the PC group. Coherently, the PC renal tissue exhibited marked elevations in IL1β, IL6, MDA and caspases alongside declines in IFN-γ, IL10 and the antioxidative enzymes GSH, CAT and GPx compared with the NC group. Furthermore, aberrant expressions of the VD metabolising enzymes, VDR and VDBP alongside a marked decrease in serum VD were detected in the PC group compared with the NC group, and the serum VD correlated inversely with the serum and renal tissue Pb.

Pb in tissues promotes the proinflammatory Th2 cytokines, IL1β and IL6, and concurrently inhibits the Th1 cytokine, IFN-γ, and the anti-inflammatory cytokine, IL10 [4,5]. Pb also provokes cellular oxidative stress by deterring the antioxidative mechanisms [6,7] and initiates cell death by stimulating Casp-8 and Casp-9 that activate the key apoptosis executor, Casp-3 [8]. Moreover, Pb dysregulates the VD endocrine system and chronic exposure in rats markedly induced the Cyp24a1 enzyme and VDBP as well as significantly downregulated VDR and Cyp27b1 in renal tissues [10,26,27,37]. The anti-inflammatory and anti-oxidative effects of VD have been characterised in the kidney and VD modulates many of the renal cytokines and anti-oxidative enzymes involved in the pathogenesis of Pb nephropathy [52–56]. Therefore, our results provide further support to the significance of inflammatory responses and oxidative stress in the pathogenesis of Pb nephropathy [4–11] and suggest that the abnormal expressions of the VD system could contribute to the pathogenesis of nephropathy by aggravating Pb-induced renal inflammation and oxidative stress [10].

The kidney and VD are pivotal for Ca^{2+} homeostasis. The TRPV5 and TRPV6 are highly selective Ca^{2+} permeable channels expressed on the apical borders of renal distal tubules (DTs) and they regulate Ca^{2+} reabsorption by the actions of VD [17–19]. CALB1 and CALB2 are intracellular CaBPs controlled by VD and are involved in the tubular Ca^{2+} reuptake [20,21]. On the other hand, Ca^{2+} contributes to renal physiology and both the $Ca_v3.1$ and $Ca_v1.2$ participate in the autoregulation of glomerular perfusion and filtration [17,22,23]. CAM/CAMKII also propagate Ca^{2+} actions in podocytes, mesangial and tubular cells [38,40]. To our knowledge, this report is the first to reveal significant inhibitions of the TRPV5, TRPV6, CALB1, CALB2, $Ca_v3.1$ and $Ca_v1.2$, whereas CAM and CAMKIIα were markedly upregulated, in the renal tissues of the PC group compared with the controls. Moreover, marked hypocalcaemia and hypercalciuria were detected, and the Ca^{2+} levels in serum, renal tissue and urine correlated inversely and significantly with those of serum and renal tissue Pb.

The dyshomeostasis in Ca^{2+} and its renal regulatory molecules could simply be a consequence of Pb nephropathy and/or the dysregulations of the renal VD system. The majority of Ca^{2+} (60–70%) is passively reabsorbed in the proximal convoluted tubules (PCT) whereas the DTs actively reabsorb about 10% of filtrated Ca^{2+} [12,13]. Although Pb was shown to inhibit the PCT Ca^{2+} reabsorption in rats [12], none of the previous studies explored the effects of Pb on the DTs active Ca^{2+} transportation. Gene deletion studies have shown that TRPV5 or TRPV6 mutant animals manifested drastic hypercalciuria and low bone density [18,19]. Others have also reported the significance of CALB1 in renal Ca^{2+} homeostasis [57]. In contrast, studies on the roles of CALB2

Table 3
Mean ± SD of renal tissue concentrations of cytokines and oxidative stress markers in the different study groups.

	NC group	PC group	Ca group	VD group	VDC group
IL-1β (pg/ml)	22.9 ± 4.5	177.3 ± 31.6[b]	101.2 ± 25.5[b,d]	90.1 ± 22.1[b,d]	33.4 ± 8.6[d,f,g]
IL-6 (pg/ml)	28 ± 4.2	221 ± 57.6[b]	71.1 ± 13.6[b,d]	57.6 ± 6.9[b,d]	44.6 ± 6.6[b,d,e]
IL-10 (pg/ml)	56.5 ± 16.6	12.4 ± 3.6[b]	29.6 ± 10[b]	39.05 ± 8.7[b,d]	147.8 ± 27[b,d,f,g]
IFN-γ (pg/ml)	138.8 ± 26.6	74.7 ± 23.7[b]	96.3 ± 14.2[b]	122.7 ± 30.4[d]	194.8 ± 34.9[b,d,f,g]
GSH (mg/g)	37.6 ± 5.6	25.3 ± 4.2[b]	30.4 ± 5.3[a]	31.6 ± 5.2[c]	40.2 ± 4.5[d,f,g]
CAT (U/mg)	253.4 ± 24	149.4 ± 23.8[b]	170.5 ± 28.7[b]	200.9 ± 32.9[b,d]	255.8 ± 20.5[d,f,g]
Gpx (μg/mg)	3.96 ± 1.06	1.94 ± 0.38[b]	2.48 ± 0.8[b]	2.52 ± 0.76[b]	3.22 ± 0.75[d]
MDA (nmol/g)	37.2 ± 5.8	49.1 ± 8.9[b]	44.01 ± 6.7	42.2 ± 6.1	38.9 ± 2.8[d]

[a] $P < 0.05$ compared with NC group.
[b] $P < 0.01$ compared with NC group.
[c] $P < 0.05$ compared with PC group.
[d] $P < 0.01$ compared with PC group.
[e] $P < 0.05$ compared with Ca group.
[f] $P < 0.01$ compared with Ca group.
[g] $P < 0.01$ compared with VD group.

Table 4
Mean ± SD of renal function parameters in the different study groups.

	NC group	PC group	Ca group	VD group	VDC group
Serum creatinine (mg/dl)	0.38 ± 0.04	0.67 ± 0.08[b]	0.55 ± 0.12[b]	0.51 ± 0.05[a,d]	0.47 ± 0.05[a,d]
Serum Urea (mg/dl)	38.1 ± 5.1	54.8 ± 6.1[b]	53.6 ± 5s.6[b]	48.2 ± 5.2[b]	36.6 ± 3.7[d,e,f]
Serum total protein (g/dl)	6.86 ± 0.57	6.15 ± 0.48[b]	6.8 ± 0.35[c]	6.88 ± 0.37[d]	6.98 ± 0.37[d]
Serum albumin (g/dl)	4.02 ± 0.43	3.18 ± 0.45[b]	3.58 ± 0.6	3.94 ± 0.73[c]	3.98 ± 0.22[d]
Urine total protein (mg/24 h)	3.41 ± 0.35	8.28 ± 1.08[b]	6.84 ± 1.01[b,c]	6.6 ± 1.19[b,d]	4.32 ± 0.91[d,e,f]

[a] $P < 0.05$ compared with NC group.
[b] $P < 0.01$ compared with NC group.
[c] $P < 0.05$ compared with PC group.
[d] $P < 0.01$ compared with PC group.
[e] $P < 0.01$ compared with Ca group.
[f] $P < 0.01$ compared with VD group.

are scarce but experimental nephrotoxicity downregulated the protein in renal tubules [20,21]. Collectively, we propose that Pb could have induced hypocalcaemia and hypercalciuria by diminishing Ca^{2+} reabsorption in the PCTs, whereas the inhibition of active VD synthesis and the downregulation of TRPV5, TRPV6, CALB1 and CALB2 in the DTs may have exacerbated the loss of Ca^{2+} in urine.

The observed abnormal expressions of the VDCCs, CAM and CAMKIIα may also participate in the pathogenesis of Pb nephropathy alongside the well-known inflammatory and oxidative stress mechanisms. In support for our hypothesis, numerous studies on nervous tissues have shown that Pb inhibits the VDCCs by competing with Ca^{2+} at the binding sites [33–35]. Others have also suggested that Pb enhanced its permeation through the VDCCs by blocking Ca^{2+} influx [36,58]. Pb also has higher affinity for CAM in relatively lower concentrations than Ca^{2+} and it activates CAM by mimicking Ca^{2+} in the EF-hand binding sites [1,24,25]. Opposingly, higher Pb concentrations induce conformational alteration and allosteric inhibition of CAM by binding to non-EF-hand sites [1,24,25]. Pb also saturated CAMKII in rat hippocampus and decreased the maximal velocity of CAMKII by 41% in the presence of Ca^{2+} and CAM [59]. Moreover, Pb nephropathy is characterised by diminished GFR, low creatinine clearance and tubular dysfunction [1,9,11]. The glomerular haemodynamics are controlled by angiotensin-II through myogenic responses that are initiated by the $Ca_v3.1$ and then maintained by the $Ca_v1.2$ [17,23]. Additionally, the simultaneous blocking of both channels increased the renal blood flow and decreased the GFR [17,22,23]. Angiotensin-II, in contrast, also induced podocyte injury and albuminuria in mice through the CAM/CAMKII pathway [60]. Furthermore, mutant mice overexpressing the active form of CAMKIIα spontaneously developed diabetic nephropathy [61], whereas the inhibition of CAMKII by a specific blocker attenuated the oxidative stress and mitochondrial dysfunction in experimental polycystic kidney disease [62]. We, therefore, hypothesis that Pb may decrease the GFR by simultaneously inhibiting the $Ca_v1.2$ and $Ca_v3.1$ in the glomerulus vasculature, thus causing concurrent dilation of the afferent and efferent arterioles and increasing the glomerular blood flow [17,22]. Pb could also have induced glomerular injury and tubular dysfunctions by over-activating the CAM/CAMKII pathway [24,25,60,61]. However, the interactions between Pb and the renal Ca^{2+}-homeostatic molecules require further research to elucidate their impacts on renal functions.

Many studies have reported ameliorative effects for Ca^{2+} supplementation against Pb toxicity [28–32]. Higher Ca^{2+} consumption than the Dietary Reference Intake lowered the BLL in postmenopausal women [26] as well as Pb levels in the blood and breast milk of pregnant and lactating women, respectively [30,32]. Ca^{2+} with or without chelators also reduced the BLL and the deposition of Pb in the tissues of pregnant rats and their suckling progenies during ongoing exposure [28,29,31]. However, Ca^{2+} therapy post-exposure to Pb showed no effect on the tissue Pb levels [28]. On the other hand, studies on the effects of VD_3 on Pb toxicity are rare. Sobel and Burger (1955) have shown that VD_3 significantly reduced the BLL and inhibited the mobilisation of Pb from bones [63]. A later study has also reported that low VD_3 intake in children was associated with higher absorption of Pb and significantly higher BLL [30]. Coherently, we have recently demonstrated antioxidative, anti-inflammatory and nephroprotective effects for prophylactic VD_3 in rats chronically exposed to Pb [10].

Herein, both monotherapies equally and significantly reduced the apoptotic index than the PC group. Ca^{2+} monotherapy, however, had negligible effects on the Pb levels and the renal biochemical and oxidative stress markers. On the contrary, VD_3 significantly decreased the serum and renal Pb levels, improved the biochemical parameters and alleviated inflammation and oxidative stress compared with both the PC and Ca groups. Our data advocates the superiority of VD_3 over Ca^{2+} in alleviating Pb-induced renal inflammation and oxidative stress, which are believed to be major mechanisms underlying the VD protective and/or therapeutic actions against a variety of renal diseases [52–56]. However, the curative efficacy of both monotherapies was moderate considering that most of the biochemical, inflammatory, oxidative stress and tissue damage markers remained significantly abnormal than the NC group. Interestingly, the dual therapy demonstrated the supreme corrective actions on all the tested parameters and the majority were also comparable between the VDC and NC groups despite maintaining Pb exposure during treatment. Consistent with our data, recent RCTs have shown that VD and Ca^{2+} co-supplementation produced boosted antioxidative and anti-inflammatory effects in diabetic patients [41] as well as in women with polycystic ovarian syndrome [42], pre-eclampsia [43] and gestational diabetes [44]. Hence, our results reinforce the notion that VD_3 and Ca^{2+} co-supplementation is associated with better anti-inflammatory and antioxidative actions [41–44], which could explicate the enhanced remedial effects of the dual therapy against Pb nephropathy.

Our data also revealed that the $Ca_v1.2$, $Ca_v3.1$, TRPV5, TRPV6, CALB1 and CALB2 were significantly upregulated with all therapeutic protocols but were generally more prominent in the VDC group. Although the different therapies also inhibited the renal expression of CAM/CAMKIIα than the PC group, both proteins remained markedly higher than the NC group. The significance of Ca^{2+}-signalling molecules in Pb nephropathy was only investigated by an earlier study that reported nephroprotection following the use of specific L-channel blockers [8]. In contrast, the present findings are aligned with those reported form the nervous system and suggest that the $Ca_v1.2$ and $Ca_v3.1$ inhibitions may participate in the pathogenesis of Pb nephrotoxicity, whereas their activation appears to be nephroprotective [33–36,58]. The controversy between the earlier report [8] and the present study could be related to differences in the experimental designs as Pb was concurrently administrated with the channel blockers and the exposure duration was relatively shorter than ours. Hence, more research is mandatory to study the relations between the renal VDCCs and Pb following acute and chronic toxicities.

The binding of Pb to the Ca^{2+} membrane and intracellular proteins

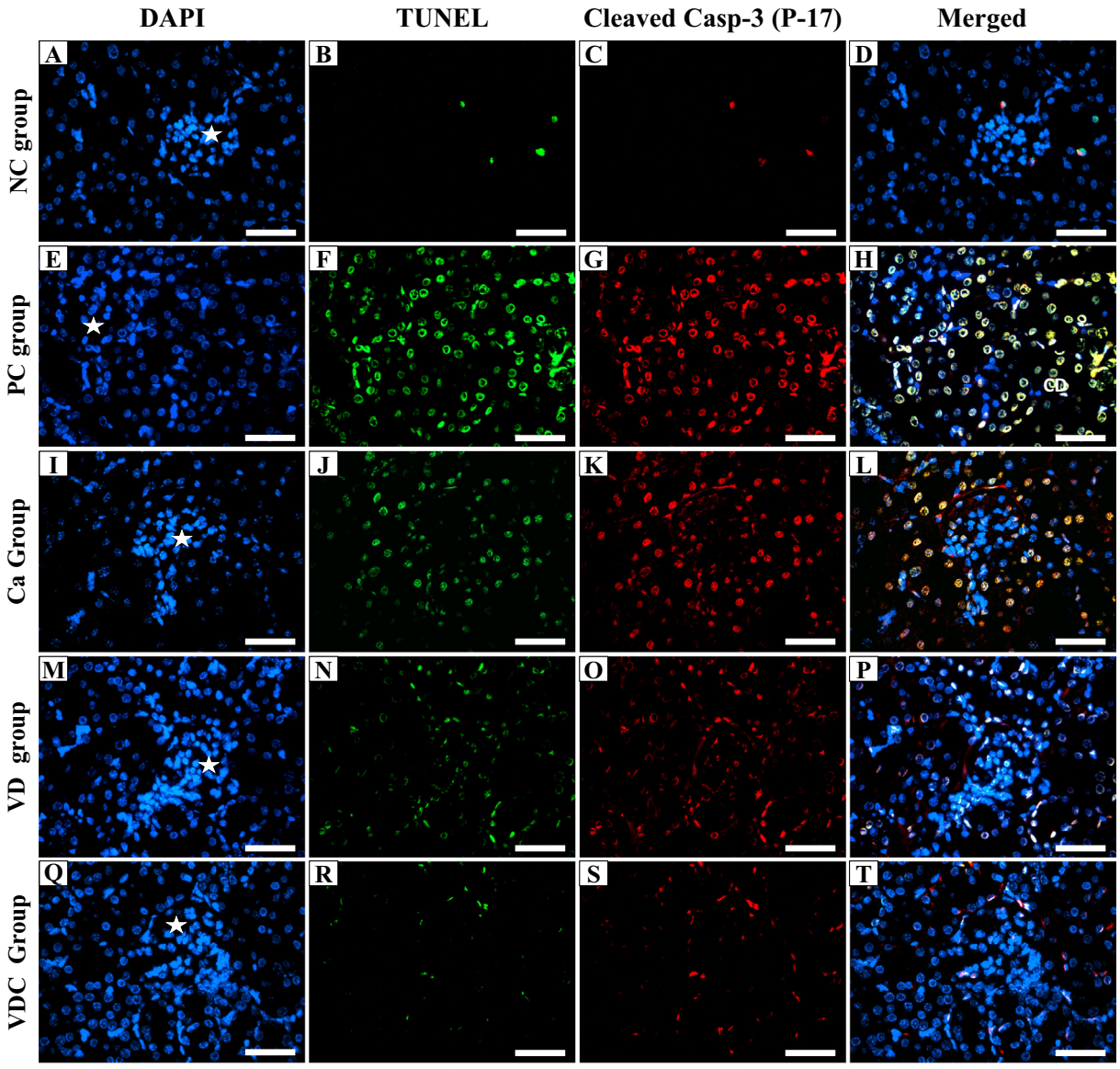

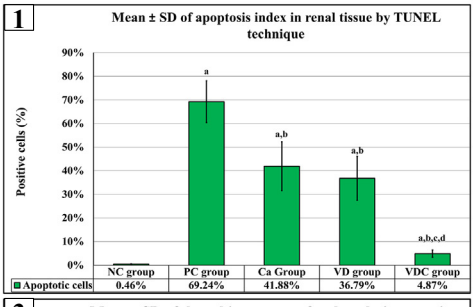

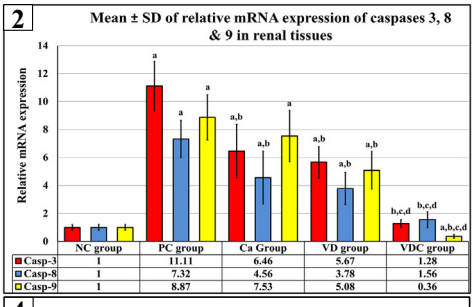

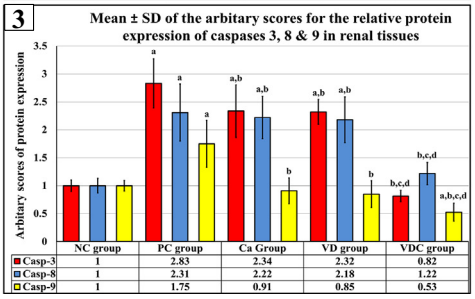

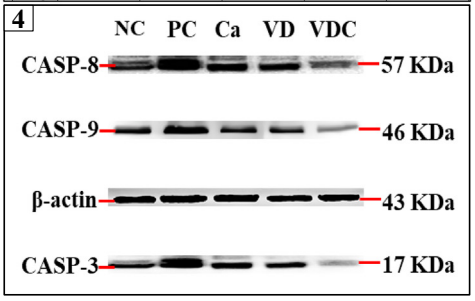

(caption on next page)

Fig. 4. Apoptotic bodies by TUNEL's technique (green) were co-localised with cleaved Casp-3 (red) by immunofluorescence in the renal tissues of NC (A to D), PC (E to H), Ca (I to L), VD (M to P) and VDC (Q to T) groups. All sections were counterstained with DAPI. (40× objective, scale bar = 15 μm and white star = glomerulus). Additionally, mean ± SD of (1) apoptosis index, (2) relative mRNA expression of caspases, (3) relative protein expression of caspases are shown as graph bars and (4) the protein expression of caspases by western blot. (a = $P < 0.05$ compared with the NC group; b = $P < 0.05$ compared with the PC group; c = $P < 0.05$ compared with Ca group and d = $P < 0.05$ compared with the VD group).

is concentration-dependent [1,24,25,64]. Moreover, VD induces Ca^{2+} influx by upregulating the VDCCs [65,66], promotes the Ca^{2+} interaction with CAM/CAMKII [67,68] as well as directly activates the CAM/CAMKII pathways [69,70]. Hence, the nephroprotective effects of the combined therapy could also involve augmenting the amount of free cytosolic Ca^{2+} by the actions of VD on Ca^{2+} influx through the $Ca_v3.1$ and $Ca_v1.2$ channels and/or Ca^{2+} mobilisation from the intracellular stores [65,66]. The escalation in the free cytosolic Ca^{2+} levels might then reach a threshold at which it would be capable of competing with and/or replacing Pb in the CAM binding sites [64–68]. Alternatively, the restoration of tubular Ca^{2+} reabsorption following the upregulations of TRPV5, TRPV6, CALB1 and CALB2 might have enhanced the tubular Pb secretion through ionic displacement mechanism(s) [2,9–11,24]. However, future *in vitro* studies are needed to measure the oscillations in cytosolic free Ca^{2+} and the tubular transportations of Ca^{2+} and Pb to verify our hypotheses.

The Cyp27b1 enzyme was atypically upregulated with the treatment modalities and reached the utmost expression in the VDC group. The enzyme production in the PCT is stimulated by the parathyroid hormone (PTH) and suppressed by VD_3 and the Fibroblast Growth Factor 23 (FGF23) [71,72]. The FGF23 is a hormone secreted by the bone and is involved in the regulation of the bone-kidney cross-talk by inhibiting the synthesis of active VD_3 and tubular phosphate (P) reabsorption [71,72]. While VD_3 stimulates the production of FGF23, the effects of PTH on the expression of FGF23 are controversial and appear to be concentration-dependent [71]. The continuous administration of PTH upregulated FGF23 due to excess bone resorption, whereas the intermittent treatment increased bone formation and diminished the FGF23 levels both *in vitro* and *in vivo* [73]. Chronic Pb intoxication, on the other hand, is manifested by increased bone resorption, elevated PTH alongside diminished VD, Ca^{2+} and P [45,46,74]. Furthermore, the removal of Pb from bones was induced by a high P diet in chronically exposed rats [63]. Currently, there is no report about the impacts of either Pb toxicity on FGF23 or chelation therapy on the PTH and blood P levels. Hence, we postulate that the atypical increase in the Cyp27b1 enzyme might be related the interactions between the PTH, VD, FGF23, bone resorption and bone minerals in relation to Pb nephropathy. In this perspective, we hypothesis that the dual therapy may have sustained bone remodelling to replace the deposited Pb in bones by Ca^{2+} and/or P through the intermittent release of PTH, which could have induced the expression of Cyp27b1 directly and/or indirectly by inhibiting the production of FGF23 [71–73]. However, further studies on the interactions between the calciotrophic hormones, Ca^{2+}, P and the bone-kidney axis with chronic Pb toxicity are indispensable to validate our supposition.

In conclusion, this study is the first to elucidate reciprocal molecular interactions between Pb nephrotoxicity and the renal VD/Ca^{2+}-homeostatic molecules that might contribute to the pathogenesis of Pb nephropathy. Additionally, VD_3 and Ca^{2+} co-supplementation appears to be an effective remedial approach against Pb nephropathy and the enhanced nephroprotective and/or restorative effects may encompass Ca^{2+}-dependent pathways that intervene with inflammation, oxidative stress and Pb metabolism. More studies are, however, still required to measure the interactions between Pb toxicity and the hormones governing the bone-kidney axis as well as the therapeutic values of the dual protocol on the other organs affected by Pb toxicity.

Supplementary data to this article can be found online at https://doi.org/10.1016/j.bbadis.2018.11.023.

Funding sources

This research did not receive any specific grant from funding agencies in the public, commercial, or not-for-profit sectors.

Competing interests

The authors declare no competing interests.

Transparency document

The Transparency document associated with this article can be found, in online version.

CRediT authorship contribution statement

Riyad A. Almaimani: Methodology, Investigation, Resources, Writing - original draft. **Hussain Almasmoum:** Methodology, Investigation, Validation, Data curation. **Mazen M. Ghaith:** Methodology, Investigation, Supervision. **Mohamed El-Boshy:** Conceptualization, Methodology, Investigation, Data curation, Supervision. **Shakir Idris:** Methodology, Validation, Investigation. **Jawwad Ahmad:** Methodology, Validation, Investigation. **Abdelghany H. Abdelghany:** Methodology, Investigation, Validation. **Mohammad A. BaSalamah:** Methodology, Investigation, Validation, Data curation. **Amani Mahbub:** Methodology, Data curation, Writing - original draft. **Bassem Refaat:** Conceptualization, Investigation, Data curation, Resources, Writing - original draft, Writing - review & editing, Supervision, Project administration.

References

[1] P. Mitra, S. Sharma, P. Purohit, P. Sharma, Clinical and molecular aspects of lead toxicity: an update, Crit. Rev. Clin. Lab. Sci. 54 (2017) 506–528, https://doi.org/10.1080/10408363.2017.1408562.
[2] I.D. de Souza, A.S. de Andrade, R.J.S. Dalmolin, Lead-interacting proteins and their implication in lead poisoning, Crit. Rev. Toxicol. 48 (2018) 375–386, https://doi.org/10.1080/10408444.2018.1429387.
[3] B.P. Lanphear, S. Rauch, P. Auinger, R.W. Allen, R.W. Hornung, Low-level lead exposure and mortality in US adults: a population-based cohort study, Lancet Public Health 3 (2018) e177–e184, https://doi.org/10.1016/s2468-2667(18)30025-2.
[4] C. Fenga, S. Gangemi, V. Di Salvatore, L. Falzone, M. Libra, Immunological effects of occupational exposure to lead (Review), Mol. Med. Rep. 15 (2017) 3355–3360, https://doi.org/10.3892/mmr.2017.6381.
[5] J. Garcia-Leston, J. Roma-Torres, O. Mayan, S. Schroecksnadel, D. Fuchs, A.O. Moreira, E. Pasaro, J. Mendez, J.P. Teixeira, B. Laffon, Assessment of immunotoxicity parameters in individuals occupationally exposed to lead, J. Toxicol. Environ. Health A 75 (2012) 807–818, https://doi.org/10.1080/15287394.2012.690327.
[6] C.M. Liu, Y.Z. Sun, J.M. Sun, J.Q. Ma, C. Cheng, Protective role of quercetin against lead-induced inflammatory response in rat kidney through the ROS-mediated MAPKs and NF-kappaB pathway, Biochim. Biophys. Acta 1820 (2012) 1693–1703, https://doi.org/10.1016/j.bbagen.2012.06.011.
[7] M. Gargouri, H. Hamed, A. Akrouti, M. Christian, R. Ksouri, A. El Feki, Immunomodulatory and antioxidant protective effect of *Sarcocornia perennis* L. (swampfire) in lead intoxicated rat, Toxicol. Mech. Methods 27 (2017) 697–706, https://doi.org/10.1080/15376516.2017.1351018.
[8] J. Zhang, H. Cao, Y. Zhang, Y. Zhang, J. Ma, J. Wang, Y. Gao, X. Zhang, F. Zhang, L. Chu, Nephroprotective effect of calcium channel blockers against toxicity of lead exposure in mice, Toxicol. Lett. 218 (2013) 273–280, https://doi.org/10.1016/j.toxlet.2013.02.005.
[9] V. Batuman, R.P. Wedeen, The persistence of chronic lead nephropathy, Am. J. Kidney Dis. 64 (2014) 1–3, https://doi.org/10.1053/j.ajkd.2014.04.004.
[10] M.A. Basalamah, A.H. Abdelghany, M. El-Boshy, J. Ahmad, S. Idris, B. Refaat, Vitamin D alleviates lead induced renal and testicular injuries by immunomodulatory and antioxidant mechanisms in rats, Sci. Rep. 8 (2018) 4853, https://doi.org/10.1038/s41598-018-23258-w.
[11] F. Harari, G. Sallsten, A. Christensson, M. Petkovic, B. Hedblad, N. Forsgard,

O. Melander, P.M. Nilsson, Y. Borne, G. Engstrom, L. Barregard, Blood lead levels and decreased kidney function in a population-based cohort, Am. J. Kidney Dis. (2018), https://doi.org/10.1053/j.ajkd.2018.02.358.
[12] L.G. Navarro-Moreno, M.A. Quintanar-Escorza, S. Gonzalez, R. Mondragon, J. Cerbon-Solorzano, J. Valdes, J.V. Calderon-Salinas, Effects of lead intoxication on intercellular junctions and biochemical alterations of the renal proximal tubule cells, Toxicol. in Vitro 23 (2009) 1298–1304, https://doi.org/10.1016/j.tiv.2009.07.020.
[13] R.T. Alexander, J. Rievaj, H. Dimke, Paracellular calcium transport across renal and intestinal epithelia, Biochem. Cell Biol. 92 (2014) 467–480, https://doi.org/10.1139/bcb-2014-0061.
[14] B. Refaat, J. Ahmad, S. Idris, F.F. Kamfar, A.M. Ashshi, S.A. Batwa, F.A. Malibary, Characterisation of vitamin D-related molecules and calcium-sensing receptor in human fallopian tube during the menstrual cycle and in ectopic pregnancy, Cell Tissue Res. 368 (2017) 201–213, https://doi.org/10.1007/s00441-016-2519-2.
[15] B. Refaat, A.G. El-Shemi, A. Ashshi, E. Azhar, Vitamin D and chronic hepatitis C: effects on success rate and prevention of side effects associated with pegylated interferon-alpha and ribavirin, Int. J. Clin. Exp. Med. 8 (2015) 10284–10303.
[16] A.H. Abdelghany, M.A. BaSalamah, S. Idris, J. Ahmad, B. Refaat, The fibrolytic potentials of vitamin D and thymoquinone remedial therapies: insights from liver fibrosis established by CCl4 in rats, J. Transl. Med. 14 (2016) 281, https://doi.org/10.1186/s12967-016-1040-4.
[17] Y. Zhou, A. Greka, Calcium-permeable ion channels in the kidney, Am. J. Physiol. Ren. Physiol. 310 (2016) F1157–F1167, https://doi.org/10.1152/ajprenal.00117.2016.
[18] J.G. Hoenderop, J.P. van Leeuwen, B.C. van der Eerden, F.F. Kersten, A.W. van der Kemp, A.M. Merillat, J.H. Waarsing, B.C. Rossier, V. Vallon, E. Hummler, R.J. Bindels, Renal Ca^{2+} wasting, hyperabsorption, and reduced bone thickness in mice lacking TRPV5, J. Clin. Invest. 112 (2003) 1906–1914, https://doi.org/10.1172/jci19826.
[19] S.D. Bianco, J.B. Peng, H. Takanaga, Y. Suzuki, A. Crescenzi, C.H. Kos, L. Zhuang, M.R. Freeman, C.H. Gouveia, J. Wu, H. Luo, T. Mauro, E.M. Brown, M.A. Hediger, Marked disturbance of calcium homeostasis in mice with targeted disruption of the Trpv6 calcium channel gene, J. Bone Miner. Res. 22 (2007) 274–285, https://doi.org/10.1359/jbmr.061110.
[20] I.Y. Chang, S.P. Yoon, The changes of calretinin immunoreactivity in paraquat-induced nephrotoxic rats, Acta Histochem. 114 (2012) 836–841, https://doi.org/10.1016/j.acthis.2012.02.005.
[21] K.Y. Kang, J.N. Kim, I.Y. Chang, S.H. Park, S.P. Yoon, Calretinin immunoreactivity in normal and carbon tetrachloride-induced nephrotoxic rats, Acta Histochem. 113 (2011) 712–716.
[22] P.B. Hansen, Functional importance of T-type voltage-gated calcium channels in the cardiovascular and renal system: news from the world of knockout mice, Am. J. Physiol. Regul. Integr. Comp. Physiol. 308 (2015) R227–R237, https://doi.org/10.1152/ajpregu.00276.2014.
[23] L.G. Navar, Intrarenal renin-angiotensin system in regulation of glomerular function, Curr. Opin. Nephrol. Hypertens. 23 (2014) 38–45, https://doi.org/10.1097/01.mnh.0000436544.86508.f1.
[24] R. Gorkhali, K. Huang, M. Kirberger, J.J. Yang, Defining potential roles of Pb(2+) in neurotoxicity from a calciomics approach, Metallomics 8 (2016) 563–578, https://doi.org/10.1039/c6mt00038j.
[25] M. Kirberger, H.C. Wong, J. Jiang, J.J. Yang, Metal toxicity and opportunistic binding of Pb(2+) in proteins, J. Inorg. Biochem. 125 (2013) 40–49, https://doi.org/10.1016/j.jinorgbio.2013.04.002.
[26] L.W. Jackson, B.A. Cromer, A. Panneerselvamm, Association between bone turnover, micronutrient intake, and blood lead levels in pre- and postmenopausal women, NHANES 1999–2002, Environ. Health Perspect. 118 (2010) 1590–1596, https://doi.org/10.1289/ehp.1002158.
[27] V. Groleau, R.A. Herold, J.I. Schall, J.L. Wagner, K.A. Dougherty, B.S. Zemel, R.M. Rutstein, V.A. Stallings, Blood lead concentration is not altered by high-dose vitamin D supplementation in children and young adults with HIV, J. Pediatr. Gastroenterol. Nutr. 56 (2013) 316–319, https://doi.org/10.1097/MPG.0b013e3182758c4a.
[28] V. Marija Varnai, M. Piasek, M. Blanusa, M. Matek Saric, D. Juresa, K. Kostial, Succimer treatment and calcium supplementation reduce tissue lead in suckling rats, J. Appl. Toxicol. 24 (2004) 123–128, https://doi.org/10.1002/jat.961.
[29] R.R. Gottipolu, C.B. Davuljigari, Perinatal exposure to lead: reduction in alterations of brain mitochondrial antioxidant system with calcium supplement, Biol. Trace Elem. Res. 162 (2014) 270–277, https://doi.org/10.1007/s12011-014-0112-7.
[30] Y.C. Hong, S.S. Kulkarni, Y.H. Lim, E. Kim, M. Ha, H. Park, Y. Kim, B.N. Kim, N. Chang, S.Y. Oh, Y.J. Kim, C. Park, E.H. Ha, Postnatal growth following prenatal lead exposure and calcium intake, Pediatrics 134 (2014) 1151–1159, https://doi.org/10.1542/peds.2014-1658.
[31] C.D. Basha, R.G. Reddy, Long-term changes in brain cholinergic system and behavior in rats following gestational exposure to lead: protective effect of calcium supplement, Interdiscip. Toxicol. 8 (2015) 159–168, https://doi.org/10.1515/intox-2015-0025.
[32] B. Gulson, K. Mizon, M. Korsch, A. Taylor, Revisiting mobilisation of skeletal lead during pregnancy based on monthly sampling and cord/maternal blood lead relationships confirm placental transfer of lead, Arch. Toxicol. 90 (2016) 805–816, https://doi.org/10.1007/s00204-015-1515-8.
[33] G. Audesirk, T. Audesirk, The effects of inorganic lead on voltage-sensitive calcium channels differ among cell types and among channel subtypes, Neurotoxicology 14 (1993) 259–265.
[34] A.K. Singh, Y. Jiang, Developmental effects of chronic low-level lead exposure on voltage-gated calcium channels in brain synaptosomes obtained from the neonatal and the adult rats, Comp. Biochem. Physiol. C: Pharmacol. Toxicol. Endocrinol. 118 (1997) 75–81.
[35] S. Peng, R.K. Hajela, W.D. Atchison, Characteristics of block by Pb^{2+} of function of human neuronal L-, N-, and R-type Ca^{2+} channels transiently expressed in human embryonic kidney 293 cells, Mol. Pharmacol. 62 (2002) 1418–1430.
[36] C. Marchetti, Role of calcium channels in heavy metal toxicity, ISRN Toxicol. 2013 (2013) 184360, https://doi.org/10.1155/2013/184360.
[37] A. Rahman, A.A. Al-Awadi, K.M. Khan, Lead affects vitamin D metabolism in rats, Nutrients 10 (2018), https://doi.org/10.3390/nu10030264.
[38] M. Bozic, J.M. Valdivielso, Calcium signaling in renal tubular cells, Adv. Exp. Med. Biol. 740 (2012) 933–944, https://doi.org/10.1007/978-94-007-2888-2_42.
[39] M. Carlstrom, C.S. Wilcox, W.J. Arendshorst, Renal autoregulation in health and disease, Physiol. Rev. 95 (2015) 405–511, https://doi.org/10.1152/physrev.00042.2012.
[40] C.M. Peppiatt-Wildman, C. Crawford, A.M. Hall, Fluorescence imaging of intracellular calcium signals in intact kidney tissue, Nephron Exp. Nephrol. 121 (2012) e49–e58, https://doi.org/10.1159/000342812.
[41] M. Tabesh, L. Azadbakht, E. Faghihimani, M. Tabesh, A. Esmaillzadeh, Calcium-vitamin D cosupplementation influences circulating inflammatory biomarkers and adipocytokines in vitamin D-insufficient diabetics: a randomized controlled clinical trial, J. Clin. Endocrinol. Metab. 99 (2014) E2485–E2493, https://doi.org/10.1210/jc.2014-1977.
[42] M. Maktabi, M. Jamilian, Z. Asemi, Magnesium-zinc-calcium-vitamin D co-supplementation improves hormonal profiles, biomarkers of inflammation and oxidative stress in women with polycystic ovary syndrome: a randomized, double-blind, placebo-controlled trial, Biol. Trace Elem. Res. 182 (2018) 21–28, https://doi.org/10.1007/s12011-017-1085-0.
[43] M. Samimi, M. Kashi, F. Foroozanfard, M. Karamali, F. Bahmani, Z. Asemi, Y. Hamidian, H.R. Talari, A. Esmaillzadeh, The effects of vitamin D plus calcium supplementation on metabolic profiles, biomarkers of inflammation, oxidative stress and pregnancy outcomes in pregnant women at risk for pre-eclampsia, J. Hum. Nutr. Diet. 29 (2016) 505–515, https://doi.org/10.1111/jhn.12339.
[44] Z. Asemi, M. Karamali, A. Esmaillzadeh, Effects of calcium–vitamin D co-supplementation on glycaemic control, inflammation and oxidative stress in gestational diabetes: a randomised placebo-controlled trial, Diabetologia 57 (2014) 1798–1806, https://doi.org/10.1007/s00125-014-3293-x.
[45] P. Alvarez-Lloret, C.M. Lee, M.I. Conti, A.R. Terrizzi, S. Gonzalez-Lopez, M.P. Martinez, Effects of chronic lead exposure on bone mineral properties in femurs of growing rats, Toxicology 377 (2017) 64–72, https://doi.org/10.1016/j.tox.2016.11.017.
[46] E. Kupraszewicz, M.M. Brzoska, Excessive ethanol consumption under exposure to lead intensifies disorders in bone metabolism: a study in a rat model, Chem. Biol. Interact. 203 (2013) 486–501, https://doi.org/10.1016/j.cbi.2013.01.002.
[47] H. Yu, T. Li, Y. Cui, Y. Liao, G. Wang, L. Gao, F. Zhao, Y. Jin, Effects of lead exposure on d-serine metabolism in the hippocampus of mice at the early developmental stages, Toxicology 325 (2014) 189–199, https://doi.org/10.1016/j.tox.2014.09.007.
[48] P. Ekambaram, V. Paul, Modulation of fluoride toxicity in rats by calcium carbonate and by withdrawal of fluoride exposure, Pharmacol. Toxicol. 90 (2002) 53–58.
[49] A.B. Nair, S. Jacob, A simple practice guide for dose conversion between animals and human, J. Basic Clin. Pharm. 7 (2016) 27–31, https://doi.org/10.4103/0976-0105.177703.
[50] S.C. Taylor, T. Berkelman, G. Yadav, M. Hammond, A defined methodology for reliable quantification of Western blot data, Mol. Biotechnol. 55 (2013) 217–226, https://doi.org/10.1007/s12033-013-9672-6.
[51] B. Refaat, A.H. Abdelghany, M.A. BaSalamah, M. El-Boshy, J. Ahmad, S. Idris, Acute and chronic iron overloading differentially modulates the expression of cellular iron-homeostatic molecules in normal rat kidney, J. Histochem. Cytochem. (2018), https://doi.org/10.1369/0022155418782696 (p. 22155418782696).
[52] S. Turk, M. Akbulut, A. Yildiz, M. Gurbilek, S. Gonen, Z. Tombul, M. Yeksan, Comparative effect of oral pulse and intravenous calcitriol treatment in hemodialysis patients: the effect on serum IL-1 and IL-6 levels and bone mineral density, Nephron 90 (2002) 188–194, https://doi.org/10.1159/000049041.
[53] M.S. Meireles, M.A. Kamimura, M.A. Dalboni, J.T. Giffoni De Carvalho, D.T. Aoike, L. Cuppari, Effect of cholecalciferol on vitamin D-regulatory proteins in monocytes and on inflammatory markers in dialysis patients: a randomized controlled trial, Clin. Nutr. 35 (2016) 1251–1258, https://doi.org/10.1016/j.clnu.2016.04.014.
[54] M. Agharazii, R. St-Louis, A. Gautier-Bastien, R.V. Ung, S. Mokas, R. Lariviere, D.E. Richard, Inflammatory cytokines and reactive oxygen species as mediators of chronic kidney disease-related vascular calcification, Am. J. Hypertens. 28 (2015) 746–755, https://doi.org/10.1093/ajh/hpu225.
[55] E. Maquigussa, C.P. Arnoni, L.G. Pereira, M.A. Boim, Calcitriol ameliorates renal damage in a pre-established proteinuria model, Mol. Med. Rep. 12 (2015) 1009–1015, https://doi.org/10.3892/mmr.2015.3555.
[56] R.B. Mustafar, R. Mohd, N.A. Miswan, A. Bain, R. Cader, A.H. Gafor, M. Mohammad, S.A. Shah, N.A. Kamaruddin, N.C. Kong, The effects of calcitriol with calcium carbonate supplementation on inflammatory biomarkers in chronic kidney disease patients' with low vitamin D, Cent. Eur. J. Immunol. 39 (2014) 236–242, https://doi.org/10.5114/ceji.2014.43729.
[57] S.H. Ko, K.C. Choi, G.T. Oh, E.B. Jeung, Effect of dietary calcium and 1,25-(OH)2D3 on the expression of calcium transport genes in calbindin-D9k and -D28k double knockout mice, Biochem. Biophys. Res. Commun. 379 (2009) 227–232, https://doi.org/10.1016/j.bbrc.2008.12.029.
[58] C.C. Hegg, V. Miletic, Chronic exposure to inorganic lead increases high-threshold voltage-gated calcium currents in rat pheochromocytoma (PC12) cells, Brain Res. 772 (1997) 63–70.

[59] C.D. Toscano, J.P. O'Callaghan, T.R. Guilarte, Calcium/calmodulin-dependent protein kinase II activity and expression are altered in the hippocampus of Pb^{2+}-exposed rats, Brain Res. 1044 (2005) 51–58, https://doi.org/10.1016/j.brainres.2005.02.076.

[60] L. Jiang, L. Xu, Y. Song, J. Li, J. Mao, A.Z. Zhao, W. He, J. Yang, C. Dai, Calmodulin-dependent protein kinase II/cAMP response element-binding protein/Wnt/beta-catenin signaling cascade regulates angiotensin II-induced podocyte injury and albuminuria, J. Biol. Chem. 288 (2013) 23368–23379, https://doi.org/10.1074/jbc.M113.460394.

[61] H. Suzuki, I. Kato, I. Usui, I. Takasaki, Y. Tabuchi, T. Oya, K. Tsuneyama, H. Kawaguchi, K. Hiraga, S. Takasawa, H. Okamoto, K. Tobe, M. Sasahara, Characterization of diabetic nephropathy in CaM kinase IIalpha (Thr286Asp) transgenic mice, Biochem. Biophys. Res. Commun. 379 (2009) 38–42, https://doi.org/10.1016/j.bbrc.2008.11.143.

[62] C. Bracken, P. Beauverger, O. Duclos, R.J. Russo, K.A. Rogers, H. Husson, T.A. Natoli, S.R. Ledbetter, P. Janiak, O. Ibraghimov-Beskrovnaya, N.O. Bukanov, CaMKII as a pathological mediator of ER stress, oxidative stress, and mitochondrial dysfunction in a murine model of nephronophthisis, Am. J. Physiol. Ren. Physiol. 310 (2016) F1414–F1422, https://doi.org/10.1152/ajprenal.00426.2015.

[63] A.E. Sobel, M. Burger, Calcification. XIII. The influence of calcium, phosphorus, and vitamin D on the removal of lead from blood and bone, J. Biol. Chem. 212 (1955) 105–110.

[64] K.A. Morales, M. Lasagna, A.V. Gribenko, Y. Yoon, G.D. Reinhart, J.C. Lee, W. Cho, P. Li, T.I. Igumenova, Pb^{2+} as modulator of protein-membrane interactions, J. Am. Chem. Soc. 133 (2011) 10599–10611, https://doi.org/10.1021/ja2032772.

[65] J.J. Bergh, Y. Shao, E. Puente, R.L. Duncan, M.C. Farach-Carson, Osteoblast Ca(2+) permeability and voltage-sensitive Ca(2+) channel expression is temporally regulated by 1,25-dihydroxyvitamin D(3), Am. J. Physiol. Cell Physiol. 290 (2006) C822–C831, https://doi.org/10.1152/ajpcell.00403.2005.

[66] A. Morelli, R. Squecco, P. Failli, S. Filippi, L. Vignozzi, A.K. Chavalmane, B. Fibbi, R. Mancina, G. Luciani, M. Gacci, E. Colli, F. Francini, L. Adorini, M. Maggi, The vitamin D receptor agonist elocalcitol upregulates L-type calcium channel activity in human and rat bladder, Am. J. Physiol. Cell Physiol. 294 (2008) C1206–C1214, https://doi.org/10.1152/ajpcell.90634.2007.

[67] S. Cheng, W.Y. So, D. Zhang, Q. Cheng, B.J. Boucher, P.S. Leung, Calcitriol reduces hepatic triglyceride accumulation and glucose output through Ca2+/CaMKKβ/AMPK activation under insulin-resistant conditions in type 2 diabetes mellitus, Curr. Mol. Med. 16 (2016) 747–758.

[68] L. Zanatta, P.B. Goulart, R. Goncalves, P. Pierozan, E.C. Winkelmann-Duarte, V.M. Woehl, R. Pessoa-Pureur, F.R. Silva, A. Zamoner, 1alpha,25-dihydroxyvitamin D(3) mechanism of action: modulation of L-type calcium channels leading to calcium uptake and intermediate filament phosphorylation in cerebral cortex of young rats, Biochim. Biophys. Acta 1823 (2012) 1708–1719, https://doi.org/10.1016/j.bbamcr.2012.06.023.

[69] M. Doroudi, Z. Schwartz, B.D. Boyan, Membrane-mediated actions of 1,25-dihydroxy vitamin D3: a review of the roles of phospholipase A2 activating protein and Ca(2+)/calmodulin-dependent protein kinase II, J. Steroid Biochem. Mol. Biol. 147 (2015) 81–84, https://doi.org/10.1016/j.jsbmb.2014.11.002.

[70] M. Doroudi, R. Olivares-Navarrete, B.D. Boyan, Z. Schwartz, A review of 1alpha,25(OH)2D3 dependent Pdia3 receptor complex components in Wnt5a non-canonical pathway signaling, J. Steroid Biochem. Mol. Biol. 152 (2015) 84–88, https://doi.org/10.1016/j.jsbmb.2015.04.002.

[71] L.D. Quarles, Role of FGF23 in vitamin D and phosphate metabolism: implications in chronic kidney disease, Exp. Cell Res. 318 (2012) 1040–1048, https://doi.org/10.1016/j.yexcr.2012.02.027.

[72] M. Koizumi, H. Komaba, M. Fukagawa, Parathyroid function in chronic kidney disease: role of FGF23-klotho axis, Contrib. Nephrol. 180 (2013) 110–123, https://doi.org/10.1159/000346791.

[73] R. Samadfam, C. Richard, L. Nguyen-Yamamoto, I. Bolivar, D. Goltzman, Bone formation regulates circulating concentrations of fibroblast growth factor 23, Endocrinology 150 (2009) 4835–4845, https://doi.org/10.1210/en.2009-0472.

[74] I. Mazumdar, K. Goswami, M.S. Ali, Status of serum calcium, vitamin D and parathyroid hormone and hematological indices among lead exposed jewelry workers in Dhaka, Bangladesh, Indian J. Clin. Biochem. 32 (2017) 110–116, https://doi.org/10.1007/s12291-016-0582-9.